New Journal of Physics
The open-access journal for physics

Cavity modes of tapered ZnO nanowires

Xiulai Xu[1,4], Frederic S F Brossard[1,5], David A Williams[1], Daniel P Collins[2], Mark J Holmes[2], Robert A Taylor[2] and Xitian Zhang[3,4]

[1] Hitachi Cambridge Laboratory, Hitachi Europe Ltd, JJ Thomson Avenue, Cambridge CB3 0HE, UK
[2] Clarendon Laboratory, University of Oxford, Oxford OX1 3PU, UK
[3] Heilongjiang Key Laboratory for Advanced Functional Materials and Excited State Processes, School of Physics and Electronic Engineering, Harbin Normal University, Harbin 150025, People's Republic of China
E-mail: xx757@cam.ac.uk and xtzhangzhang@hotmail.com

New Journal of Physics **12** (2010) 083052 (7pp)
Received 24 May 2010
Published 25 August 2010
Online at http://www.njp.org/
doi:10.1088/1367-2630/12/8/083052

Abstract. We report on a cavity mode mapping of ZnO tapered nanowires using micro-photoluminescence spectroscopy at room temperature. Both the Fabry–Perot (FP) and the whispering gallery (WG) modes are identified in a single wire. The emission spectra from single nanowires comprise regular Lorentzian peaks, which arise from the FP interference between the ends of the nanowire. The overall intensity along the tapered wire varies periodically. This variation is ascribed to WG mode resonances across the nanowire. The results agree well with the theoretical calculations using the finite-difference time-domain method.

Contents

[4] Authors to whom any correspondence should be addressed.
[5] Equally contributing first authors.

1. Introduction

ZnO nanowires have attracted much interest because of their large exciton binding energy, which enables the exciton to remain stable at room temperature. Many applications have been investigated, such as field effect transistors, photo detectors, lasers, piezoelectric nanogenerators and diluted magnetic semiconductors [1]–[4]. In particular, the excitonic transition has a large oscillator strength, which provides the possibility of achieving strong exciton–photon coupling [5, 6]. Because of the structure of a ZnO nanowire, there are two cavity modes that can be observed, namely the Fabry–Perot (FP) and the whispering gallery (WG) modes. FP cavity modes can be observed easily because of the reflection from the two nanowire or nanobelt ends [7]. WG modes have been investigated in hexagonal ZnO microdiscs in order to observe lasing effects [8]–[14]. WG modes or FP modes across a tapered ZnO nanowire have been investigated using second harmonic generation microscopy [15, 16]. In photoluminescence (PL) measurements, however, multiple modes are excited, which makes mode analysis more complicated. In the present study, cavity modes of the tapered ZnO nanowires are mapped using confocal micro-PL spectroscopy. Both FP and WG modes are observed in single tapered nanowires. The finite-difference time domain (FDTD) technique is used to simulate the cavity modes.

2. Experimental details

The vapour transport process was used to synthesize ZnO nanowires [17, 18]. An In/ZnO mixture was loaded at one end of an alumina boat, and a 2 nm Au-coated Si substrate was put at the other end of the boat, downstream of the mixture. The boat was loaded into the centre of a horizontal furnace. The nanowires were grown at 1400 °C under flowing nitrogen gas, with a flow rate of 30 ml min^{-1} and a partial pressure of 50 Pa. More details of the growth can be found in [17, 18]. The length of the nanowires can be up to 30 μm and the diameters vary from 100 to 400 nm. The structure of the nanowires has been investigated using x-ray diffraction, which confirms the wurtzite ZnO phase [18]. The nanowires were transferred from the substrate and dispersed in isopropyl alcohol. They were then spin-coated onto an Si wafer with 200 nm of SiO_2 on the surface. The position of the nanowires was identified using a scanning electron microscope (SEM) aided by pre-patterned registration marks. Figure 1(a) shows an SEM image of one nanowire and the cross section of the small end of the wire is shown in the inset. In this work, two nanowires are investigated. One wire has a diameter varying from 500 to 160 nm with a length of 13.5 μm (W1), as shown in figure 1(a), and the other straight wire has a diameter of 400 nm with a length of 9 μm (W2).

The photoluminescence (PL) measurements from single wires were performed using a conventional micro-PL system. The excitation source for the PL was a frequency-tripled 100 fs Ti:sapphire laser producing excitation pulses at 266 nm. The laser power was 84 μW. The pump laser light was focused in a direction normal to the wire, using a $\times 36$ reflective microscope objective suitable for the ultraviolet range, to a spot size of ~ 2 μm diameter. The objective was mounted on an xyz piezoelectric stage with 20 μm travel along each axis and 1 nm resolution. The PL mapping was done by moving the objective position over the wire surface. The light emitted from the nanowires was collected with the same objective and dispersed through a 0.3 m monochromator, and then it was detected with a cooled charge-coupled device camera. A linear polarizer was placed in front of the monochromator for polarization measurements.

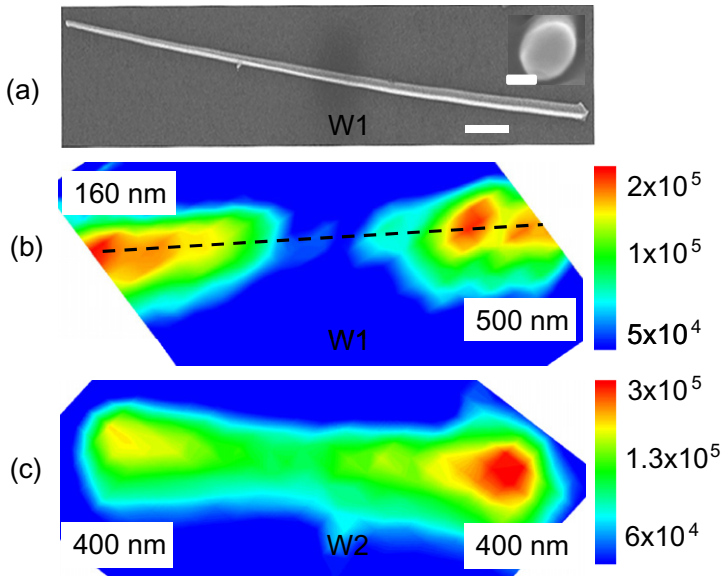

Figure 1. (a) SEM image of a single tapered ZnO nanowire. The white scale bar is 1 μm. Inset: an image of one end of the wire. Here the white scale bar is 100 nm. (b and c) Contour plots of the overall PL intensity of W1 and W2, respectively. The scanning areas for panels (b) and (c) are 5×15 and $6 \times 12\,\mu\text{m}^2$, respectively. The scale bars indicate the intensity of the PL in arbitrary units.

3. Results and discussion

The PL emission shows a broad peak between 360 nm and 450 nm, which is due to band edge emission [7, 15, 19, 20]. The overall PL intensities at the band edge of W1 and W2 are plotted in figures 1(b) and (c), respectively. The polarization of emitted light is mainly along the wire for both cases [21]. It can be seen that the intensity at the ends of the nanowires is enhanced, which is ascribed to an enhancement by the FP modes between the ends of the wire. This is similar to what we observed in ZnO nanobelts [7]. Interestingly, for the tapered wire in figure 1(b), the intensity varies in a nearly periodic manner with a period of a few microns. This was systematically observed in all tapered wires.

Figure 2(a) shows the PL spectra along the nanowire W1. The maximum intensity shifts from higher to lower energy when the laser spot moves from the small end to the large end of the nanowires, unlike the case of the straight nanowire W2. We ascribe this shifting to the WG modes across the wire [22]. In addition, the broad band edge emission peak at about 390 nm comprises several peaks. These peaks can be fitted with a Lorentzian function, as shown by the green lines in figure 2(b) for the general case of W1. A similar multi-peak feature has been observed in the straight nanowire and in nanobelts [7], which we believe is due to the presence of standing-wave FP modes along the nanowire. It can be seen that the peak separations increase with the emission wavelength, due to the dispersion in this wavelength regime. In the ideal case of an FP cavity, the longitudinal mode spacing is determined by $\Delta\lambda_c = \frac{\lambda_1\lambda_2}{2nL}$, where n is the effective refractive index, L is the length of the cavity, and λ_1 and λ_2 are the two adjacent peaks. With the observed separations, the deduced effective cavity length L is $\sim 9\,\mu$m when $n = 2.4$

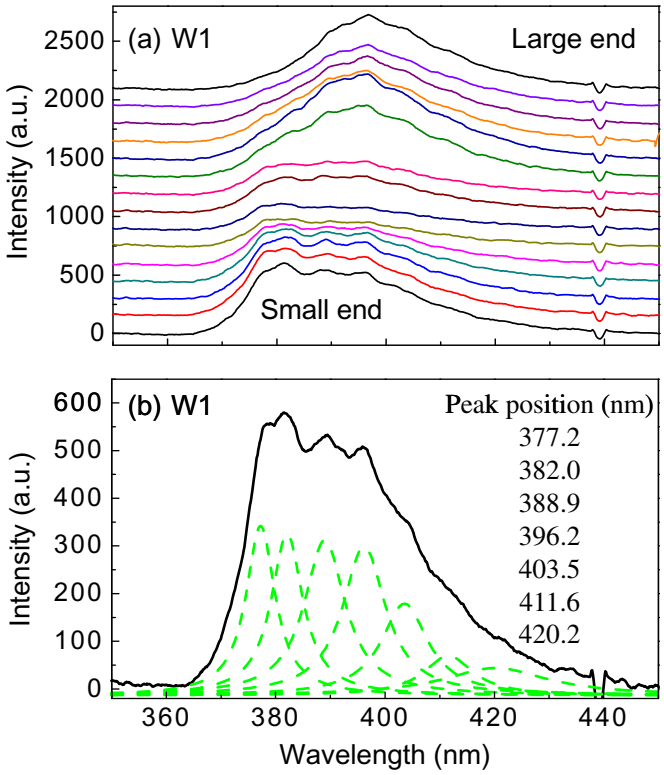

Figure 2. (a) PL spectra along W1, as shown by the dashed line in figure 1(b). The spectra are shifted for clarity. (b) A typical PL spectrum from W1. The green lines (dashed) are fitted spectra with a Lorentzian line shape.

for the straight wire W2, which agrees well with what we measured with the SEM. However, for the tapered nanowire W1, the calculated cavity length is $\sim 6.3\,\mu$m, which is shorter than the measured length. This is probably due to the fact that the effective refractive index is lower than 2.4 for the guided modes in the tapered nanowire. For the tapered wire W1, we only have three guided modes (HE_{11}, TE_{01} and TM_{01}), which can propagate along the entire length of the wire without being cut off and contribute to the FP standing wave in figure 2(b). The effective refractive index for these guided modes can be as low as 1.1 for a ZnO nanowire of diameter 150 nm [23]. Other possible reasons for the effective short length calculated can be due to the tapering and the irregular wire end facets.

Intensity oscillations of second harmonic generation along the ZnO nanowire/nanorods have been explained with either FP modes across the wire with a perfect hexagonal cross section [15] or second harmonic WG modes [16]. In our case, there are no FP modes across the wire because the cross section is not hexagonal, as shown in the inset of figure 1(a). In order to fully understand the PL intensity mapping, we used the FDTD technique to find the WG modes with a freely available software package (MEEP) [24, 25]. For a circular cavity, both TE and TM modes can be numbered by two integer mode numbers m ($\geqslant 0$) and l ($\geqslant 1$), which are defined by the angular and radial mode patterns [11, 26]. We first calculated the resonance frequencies (normalized to the diameter) of the WG modes in a two-dimensional (2D) circular cavity. The radial mode number l was identified from the mode profile and TE/TM modes selected depending on the polarization of a Gaussian pulse source located inside the cavity and off-centred. We deduce the spatial position of the WG modes along the nanowire W1

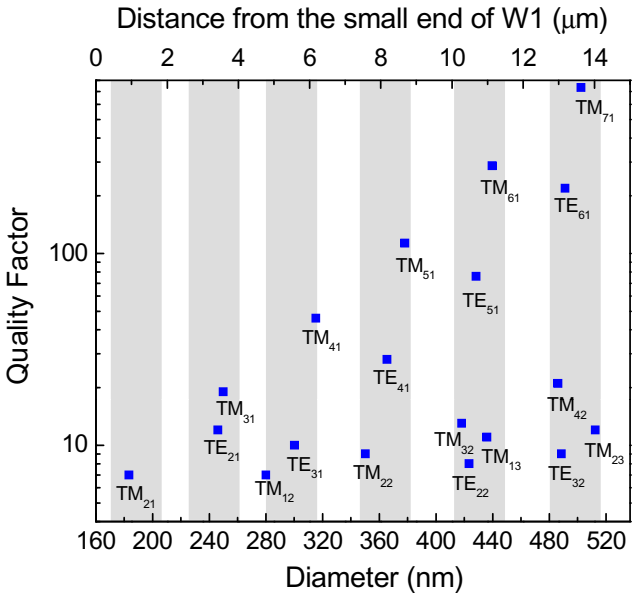

Figure 3. Quality factors of WG modes as a function of wire diameter with an emission wavelength at 390 nm using the FDTD method. The grey stripes (used to guide the eyes) with a width of 1.5 μm illustrate the intensity spreading with a full-width at half-maximum of the PL spectrum of 40 nm.

from the calculated diameter considering a light emission wavelength of 390 nm, as shown in figure 3. It is clear that the larger section of the wire supports an increase in the number of WG resonances with higher azimuthal and radial mode numbers, as expected. We observe that the WG modes are grouped together. For example, the resonant diameter for TM_{31} is close to that for TE_{21}, which has been observed previously [11]. Most of them occur within a distance too small to resolve with our optical setup: the spatial resolution is in part limited by the laser spot size (2 μm) and the spectral width of our internal light source exciting the WG modes, about 40 nm as measured from the PL spectrum. The latter figure translates into a spatial width of about 1.5 μm along the tapered wire, which we illustrate by the grey regions in figure 3. We have also reported in figure 3 the quality factor (Q) obtained from the above FDTD calculation without considering the absorption [27]. We note that the mode with the highest Q in each group is of $TM_{m,l}$ type with $l = 1$, while modes with $l > 1$ have a very low Q (below 20).

To confirm our findings, we performed an FDTD calculation on a tapered circular nanowire with the same dimensions of W1. The guided modes and WGM supported by the wire were excited with a point source (dipole) with an optical width corresponding to that from the experiment. The point source is located inside but close to the surface of the nanowire with the electric field polarized along the nanowire axis. The source was left to decay and the fields monitored over 200 periods to allow the guided modes to probe the ends of the wire. The total electric and magnetic energy was integrated over a few periods. An example of the resulting energy distribution across the wire is given in figure 4(a) for $m = 3$, where TM_{31} TM_{32}, TE_{31} and TE_{32} can be clearly observed. The spatial positions of the energy maxima emitted into free space along the wire match well with those obtained in figure 3 for the WGM of the same order.

The computation and mode identifications were repeated for each mode number m between 0 and 6 and combined to produce figure 4(b). Figure 4(c) is the intensity obtained from a line

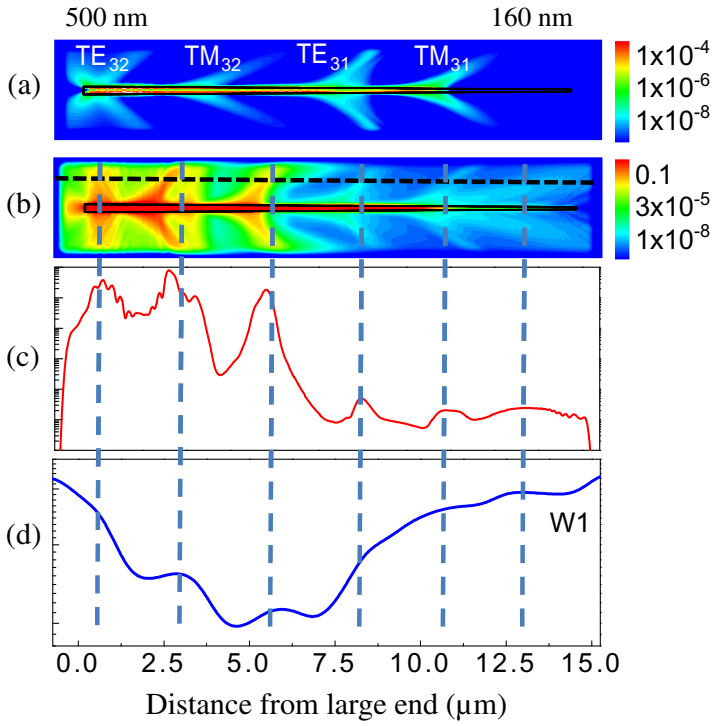

Figure 4. (a) Simulated field intensity distribution for WG modes when $m = 3$ and (b) superimposed m from 0 to 6 with dimensions identical to W1, as shown in the centre. The scale bar indicates the intensity of the PL in arbitrary units. (c) Simulated intensity profile along the nanowire modelled in (b). (d) Experimentally measured intensity profile from W1 in figure 1(b). The dark blue dashed lines are used to guide the eyes.

scan of the energy distribution above the wire, as shown in figure 4(b), which we compare with that obtained in figure 1(b). Due to the closely spaced modes, only six main energy maxima are obtained in both cases with similar spacing between the modes. In our FDTD method, we believe that the $TM_{m,l}$ modes produce the intensity variations measured along the wire in figure 4(d) due to the higher Q. The diameters corresponding to the intensity maxima in figure 4(d) are not located exactly at the positions of the simulated ones. This could be ascribed to the non-perfect tapering of the wire and material dispersion. Another reason for the discrepancies could be because of the accuracy of the measurement setup with a laser spot size of 2 μm. In fact, the laser beam profile is also deformed during the measurement when the objective is moving. We note that the overall intensity at the small end is stronger in the experiment than in the model, as we observed in nanobelts [7]. This is because more luminescence is scattered without guiding at the excitation spot in the experiment for small nanorod diameters, and because emission from the end of the wire is also collected.

4. Conclusion

In summary, cavity modes from tapered nanowires have been mapped by micro-PL spectroscopy. Both the FP and the WG modes have been observed in these wires. The emission

intensities are enhanced at the end of the nanowires because of FP interference, resulting in a multi-peak feature in the spectrum. In addition, the maximum intensity shifts to a shorter wavelength when the diameter decreases along the wire due to the presence of WG cavity modes. The WG modes have been simulated by the FDTD technique. The simulated results agree well with experimental observations.

References

[1] Ozgur U, Alivov Y I, Liu C, Teke A, Reshchikov M A, Dogan S, Avrutin V, Cho S-J and Morkoc H 2005 *J. Appl. Phys.* **98** 041301
[2] Lu M P, Song J, Lu M Y, Chen M T, Gao Y, Chen L J and Wang Z L 2009 *Nano Lett.* **9** 1223
[3] Yang P, Yan H, Mao S, Russo R, Johnson J, Saykally R, Morris N, Pham J, He R and Choi H J 2003 *Adv. Funct. Mater.* **12** 323
[4] Lu W and Lieber C M 2006 *J. Phys. D: Appl. Phys.* **39** R387
[5] van Vugt L K, Ruhle S, Ravindran P, Gerritsen H C, Kuipers L and Vanmaekelbergh D 2006 *Phys. Rev. Lett.* **97** 147401
[6] Sun L, Chen Z, Ren Q, Yu K, Bai L, Zhou W, Xiong H, Zhu Z Q and Shen X 2008 *Phys. Rev. Lett.* **100** 156403
[7] Xu X L, Brossard F S F, Williams D A, Collins D P, Holmes M J, Taylor R A and Zhang X 2009 *Appl. Phys. Lett.* **94** 231103
[8] Ursaki V V, Burlacu A, Rusu E V, Postolake V and Tiginyanu I M 2009 *J. Opt. A: Pure Appl. Opt.* **11** 075001
[9] Zhang C F, Zhang F, Sun X W, Yang Y, Wang J and Xu J 2009 *Opt. Lett.* **34** 3349
[10] Wiersig J 2003 *Phy. Rev.* A **67** 023807
[11] Nobis T and Grundmann M 2005 *Phy. Rev.* A **72** 063806
[12] Liu J, Lee S, Ahn Y H, Park J Y, Koh K H and Park K H 2008 *Appl. Phys. Lett.* **92** 263102
[13] Zhu G P, Xu C X, Zhu J, Lv C G and Cui Y P 2009 *Appl. Phys. Lett.* **94** 051106
[14] Wang D, Seo H W, Tin C-C, Bozack M J, Williams J R, Park M and Tzeng Y 2006 *J. Appl. Phys.* **99** 093112
[15] Mehl B P, House R L, Uppal A, Reams A J, Zhang C, Kirschbrown J R and Papanikolas J M 2010 *J. Phys. Chem.* A **114** 1241
[16] Zhang Y, Zhou H, Liu S W, Tian Z R and Xiao M 2009 *Nano Lett.* **9** 2109
[17] Zhang X, Lu H, Gao H, Wang X, Xu H, Li Q and Hark S 2009 *Cryst. Growth Des.* **9** 364
[18] Wu L, Zhang X, Wang Z, Liang Y and Xu H 2008 *J. Phys. D: Appl. Phys.* **41** 195406
[19] Ruhle S, van Vugt L K, Li H-Y, Keizer N A, Kuipers L and Vanmaekelbergh D 2008 *Nano Lett.* **8** 119
[20] Xu X L, Lau S P, Chen J S, Chen G Y and Tay B K 2001 *J. Cryst. Growth* **223** 201
[21] Wang J, Guidiksen M S, Duan X, Cui Y and Lieber C M 2001 *Science* **293** 1455
[22] Nobis T, Kaidashev E M, Rahm A, Lorenz M and Grundmann M 2004 *Phys. Rev. Lett.* **93** 103903
[23] Henneghien A L, Gayral B, Desieres Y and Gerard J-M 2009 *J. Opt. Soc. Am.* B **26** 2396
[24] Farjadpour A, Roundy D, Rodriguez A, Ibanescu M, Bermel P, Joannopoulos J D, Johnson S G and Burr G 2006 *Opt. Lett.* **31** 2972
[25] Oskooi A F, Roundy D, Ibanescu M, Bermel P, Joannopoulous J D and Johnson S G 2010 *Comput. Phys. Commun.* **181** 687
[26] Maslov A V, Bakunov M I and Ning C Z 2006 *J. Appl. Phys.* **99** 024314
[27] Yoshikawa H and Adachi S 1997 *J. Appl. Phys.* **36** 6237